Available online at www.sciencedirect.com
ScienceDirect
Global and Planetary Change 56 (2007) 83–100
GLOBAL AND PLANETARY CHANGE
www.elsevier.com/locate/gloplacha

Distributed modelling of the regional climatic equilibrium line altitude of glaciers in the European Alps

Michael Zemp *, Martin Hoelzle, Wilfried Haeberli

Glaciology and Geomorphodynamics Group, Department of Geography, University of Zurich, Winterthurerstr. 190, CH-8057 Zurich, Switzerland

Received 9 August 2005; accepted 21 July 2006
Available online 11 September 2006

Abstract

Glaciers are among the key indicators of ongoing climate change. The equilibrium line altitude is a theoretical line which defines the altitude at which annual accumulation equals the ablation. It represents the lowest boundary of the climatic glacierisation and, therefore, is an excellent proxy for climate variability. In this study we introduce a simple approach for modelling the glacier distribution at high spatial resolution over entire mountain ranges using a minimum of input data. An empirical relationship between precipitation and temperature at the steady-state equilibrium line altitude (ELA_0), is derived from direct glaciological mass balance measurements. Using geographical information systems (GIS) and a digital elevation model, this relationship is then applied over a spatial domain, to a so-called distributed modelling of the regional climatic ELA_0 ($rcELA_0$) and the climatic accumulation area (cAA) of 1971–1990 over the entire European Alps. A sensitivity study shows that a change in $rcELA_0$ of ±100 m is caused by a temperature change of ±1 °C or a precipitation decrease of 20% and increase of 27%, respectively. The modelled cAA of 1971–1990 agrees well with glacier outlines from the 1973 Swiss Glacier Inventory. Assuming a warming of 0.6 °C between 1850 and 1971–1990 leads to a mean $rcELA_0$ rise of 75 m and a corresponding cAA reduction of 26%. A further rise in temperature of 3 °C accompanied by an increase in precipitation of 10% leads to a further mean rise of the $rcELA_0$ of about 340 m and reduces the cAA of 1971–1990 by 74%.

Keywords: glacier; climate at equilibrium line altitude; climate change; geographical information systems

1. Introduction

Fluctuations of mountain glaciers are among the best natural indicators of climate change (IPCC, 2001). Glacier mass balance is the direct and undelayed signal of annual atmospheric conditions, i.e., temperature, precipitation and radiation balance (Haeberli, 2004). The equilibrium line altitude (ELA) on a glacier is a theoretical line which defines the altitude at which annual accumulation equals the ablation. It represents the lowest boundary of climatic glacierisation — that is, where glacierisation can begin. Thus, climatic variability can be inferred from variations in the ELA (Kuhn, 1981; Ohmura et al., 1992; Lie et al., 2003a).

To understand the climate at the ELA the processes of accumulation and ablation can be examined, the latter based on the energy balance principle. Another approach is to search for relationships between the relevant parameters for the ELA and the glacier accumulation or ablation (Ahlmann, 1924; Shumsky, 1964; Ohmura et al., 1992).

Physical models describing the relationship between glacier behaviour and climate change can be very

* Corresponding author.
E-mail address: mzemp@geo.unizh.ch (M. Zemp).

0921-8181/$ - see front matter © 2006 Elsevier B.V. All rights reserved.
doi:10.1016/j.gloplacha.2006.07.002

sophisticated (Greuell, 1989; Klok and Oerlemans, 2002), in particular those which include the mechanics of glacier flow, driven by the mass balance (e.g., Leysinger Vieli and Gudmundsson, 2004). These models require detailed input data from various sources. Because of their complexity, they facilitate a deeper understanding of physical glacier behaviour (Kerschner, 2002). However, due to the large amount of required input data, they can be applied only to recent glacier states and to single glaciers or glacierised catchments. Other studies use correlations between glacier energy balance, ablation and meteorological parameters to complete and extend mass balance series in time (e.g., Hoinkes and Steinacker, 1975; Braithwaite, 1981; Letréguilly and Reynaud, 1990).

Our aim is a) to present a simple approach that is able to model the glacier distribution at high spatial resolution (about 100 m) over entire mountain ranges, b) to investigate the sensitivity of the Alpine[1] glacierisation to changes in temperature and precipitation, and c) to demonstrate the possible impact of a climate scenario on Alpine glacierisation in the decades to come. To achieve this, an empirical relationship between precipitation and temperature at the steady-state equilibrium line altitude (ELA_0) is derived from direct glaciological mass balance measurements. GIS techniques and a DEM are then used to apply this relationship over a spatial domain to a so-called distributed modelling of the regional climatic ELA_0 ($rcELA_0$), and the climatic accumulation area (cAA) of 1971–1990 over the entire European Alps. Different sources of model errors and the order of magnitude of their amounts are discussed. In conclusion, a sensitivity study demonstrates the potential of this distributed modelling approach for the reconstruction of historical $rcELA_0$ and future scenarios.

2. Previous studies

In the relevant literature, and in the various languages used there, no consistent terminology can be found for the equilibrium line altitude. Gross et al. (1978) gave an overview of definitions of glacier snowline, firn line, equilibrium line and different approaches for estimating these. In this study we use the original terms cited in the literature. In addition, we distinguish between equilibrium line altitude (ELA), steady-state equilibrium line altitude (ELA_0), regional climatic equilibrium line altitude ($rcELA_0$) and local topographic equilibrium line altitude ($ltELA_0$).

[1] In this article 'Alps' or 'Alpine' refer explicitly to the European Alps, the terms 'alps' or 'alpine' are purely generic.

Haeberli (1983) presented a schematic diagram of glacier limits after Shumsky (1964), describing the distribution of glaciers primarily as a function of mean annual air temperature and annual precipitation. As a general rule, in humid-maritime regions, the ELA is at low altitude because of the great amount of ablation required to eliminate the deep snowfall. Temperate glaciers dominate these landscapes. Such ice bodies, with relatively rapid flow, exhibit a high mass turnover and react strongly to atmospheric warming by enhanced melt and runoff. Under dry continental conditions the ELA is at high elevation. In such regions, glaciers are polythermal or cold and feature a low mass turnover.

The basic idea of discovering an empirical relationship between precipitation or temperature and the snowline goes back to Ahlmann (1924). Krenke (1975) pursued a similar concept for estimating precipitation in high mountain areas in the former Soviet Union. Ananicheva and Krenke (2005) used such relationships to investigate the evolution of the climatic snowline and the ELA in north-eastern Siberia Mountains. Gross et al. (1978) suggested a steady-state Accumulation Area Ratio (AAR_0) of 0.67 for glaciers in the Alps as an approximation of the ELA_0 and zero mass balance and compared it to the eight most frequently applied methods for the estimation of the snowline. Furthermore they used the AAR_0 to estimate the snowline depression of Late-Würm (20,000–10,000 years BP) glacier readvances. With the AAR_0 method, the ELA_0 of past glaciers is fairly easy to determine from topographical glacier maps and hence often applied in palaeo-climatic studies (e.g., Kerschner, 1985; Maisch, 1992; Kerschner et al., 2000; Maisch et al., 2000). However, AAR_0 values obtained from worldwide mass balance measurements vary between 0.22 and 0.72 (IUGG(CCS)/UNEP/UNESCO/WMO, 2005). Therefore, the AAR_0 method should not be used uncritically.

Multivariate regression models, relating the change in the dependent variable (ELA) to the changes in the independent variables (climate data) were presented by Ohmura et al. (1992), Kerschner (1996) and Greene et al. (1999). The results of the multivariate regression analysis are difficult to interpret from a physical point of view and, for statistical reasons, are of only limited value for extrapolation beyond the spatial and temporal limits of the independent variables in the original data set (Kerschner, 1996).

Shea et al. (2004) modelled a simple cell-based climatology of the Canadian Rockies from temperature, precipitation and snowfall lapse rates constructed from climate normal, and elevation attributes extracted from a 1-km DEM for the period 1961–1990. Fractional

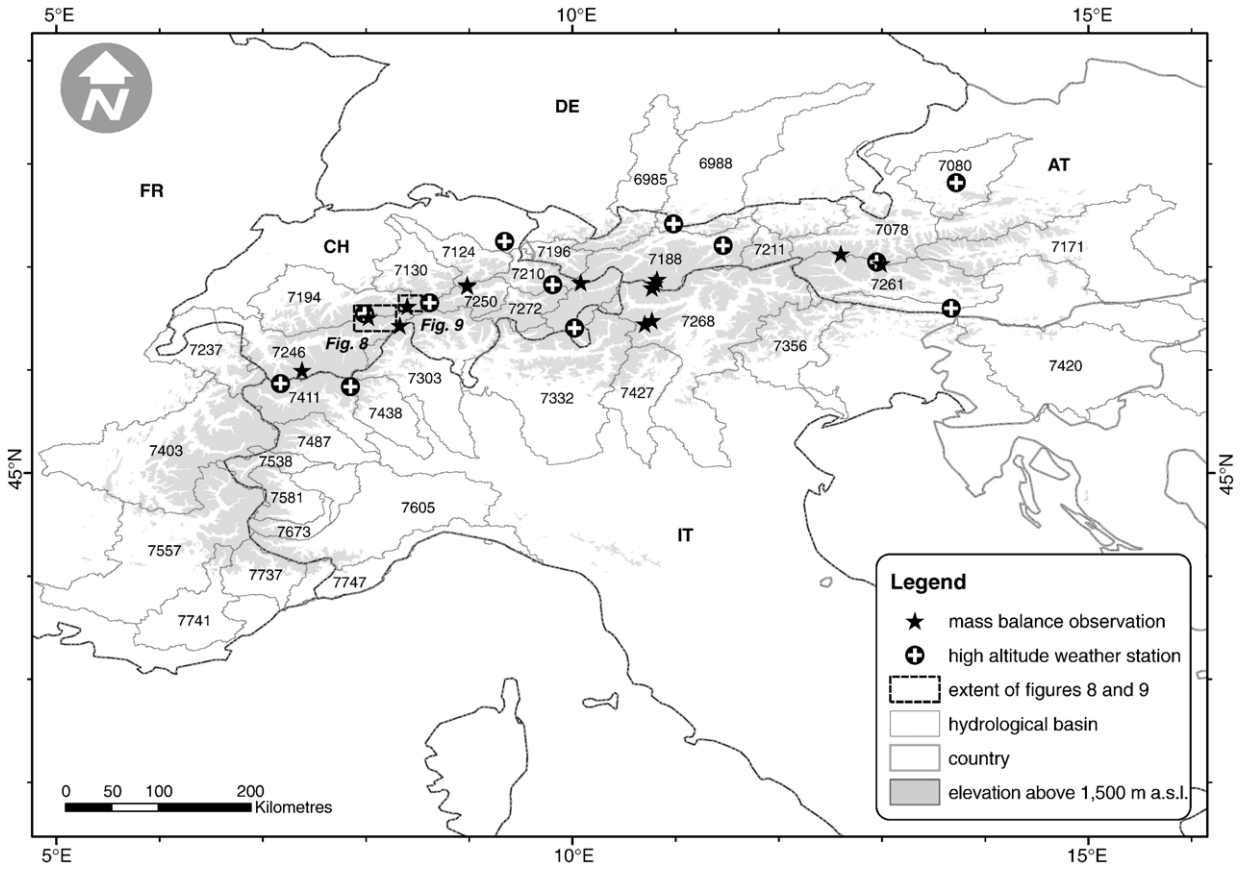

Fig. 1. Alpine mountain range (shaded in grey) with available mass balance observations (glaciers from west to east: Giétro, Grosser Aletsch, Gries, Rhone, Limmern, Plattalva, Silvretta, Caresèr, Fontana Bianca, Hintereis, Kesselwand, Vernagt, Sonnblick and Wurten) and high altitude weather stations (from west to east: Gr. St. Bernhard, Lago Gabiet, Junfraujoch, Gütsch ob Andermatt, Säntis, Weissfluhjoch, Bernina Hospiz, Zugspitze, Patscherkofel, Sonnblick, Villacher Alpe and Feuerkogel). Hydrological basins from the HYDRO1k DEM (http://LPDAAC.usgs.gov) are labelled with the corresponding basin IDs. The spatial extent of Fig. 8 and 9 is indicated by dashed black lines.

glacierised areas were calculated from a digital glacier inventory for the 0.25°×0.5° model cells. Single and multivariate statistical analysis was then performed to determine the climatic variables controlling the spatial distribution of glaciers in the Rockies.

Lie et al. (2003a) presented an exponential relationship between mean ablation season temperature and winter precipitation at the ELA of ten Norwegian glaciers. Using interpolated precipitation and temperature data for the period of 1961–1990 and a DEM of southern Norway, they modelled the altitude of instantaneous glacierisation (AIG) and the corresponding glacier accumulation areas, with a spatial resolution of 5° min (Lie et al., 2003b).

The approach presented in this study is based on the concept of Haeberli (1983) and Shumsky (1964). We present an empirical relationship between 6-month summer temperature and annual precipitation at the ELA_0, based on the period of 1971–1990. Rather than applying the often-used AAR_0 method, we determine the ELA_0 from direct glaciological mass balance measurements. Implementing the approach from Lie et al. (2003a), we then apply the obtained empirical relationship, using GIS techniques, to

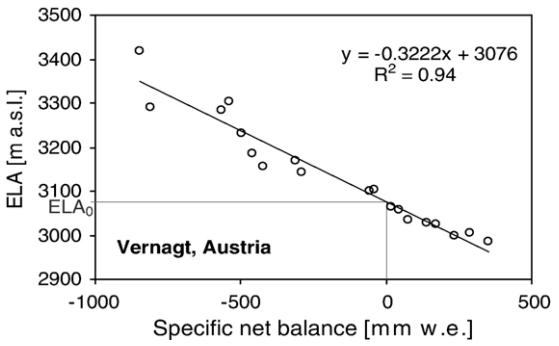

Fig. 2. Linear relationship between ELA and specific net balance of Vernagt Glacier (Austria) for the period 1971–1990. The ELA_0 of 3076 m a.s.l. represents the calculated ELA value for a zero net balance, i.e., a hypothetical steady-state.

model the AIG, the rcELA$_0$ and the cAA with a spatial resolution of 3 arc sec (approx. 100 m) over the entire European Alps.

3. Methods

In Fig. 1 an overview is given of all the elements mentioned later in the article, such as locations of mass balance observations, high altitude weather stations, hydrological basins and extent of the Alpine mountain range.

3.1. Precipitation and temperature at the ELA$_0$

To set up an empirical relationship between precipitation and temperature at the ELA$_0$ we focus on the period of 1971–1990. In this period, mass balance series from 14 Alpine glaciers as well as Alpine-wide temperature and precipitation data are available. The ELA$_0$ is calculated for each glacier from the relation between the specific net balance and the ELA, as compiled by the World Glacier Monitoring Service (http://www.wgms.ch) and published in the Glacier Mass Balance Bulletin series (e.g. IUGG(CCS)/UNEP/UNESCO/WMO, 2005). ELA values outside the glacier altitude range (i.e., when the entire glacier is an accumulation or ablation area) are excluded in this regression analysis. Fig. 2 shows the example of Vernagt Glacier (Austria) with an ELA$_0$ of 3076 m a.s.l. The regression analysis of the 14 glaciers shows coefficients of determination (R^2) ranging from 0.74 to 0.99, with a mean of 0.89.

Precipitation values at the glacier ELA$_0$ were obtained from the Alpine precipitation climatology (1971–1990) published by Frei and Schär (1998) and Schwarb et al. (2001). Based on a comprehensive database with observations from 5831 conventional rain gauges and 259 totalisators (i.e. cumulative precipitation gauges), this gridded data set provides mean monthly precipitation (1971–1990), as well as monthly precipitation–elevation gradients on a spatial resolution of 1.25 arc min (approx.

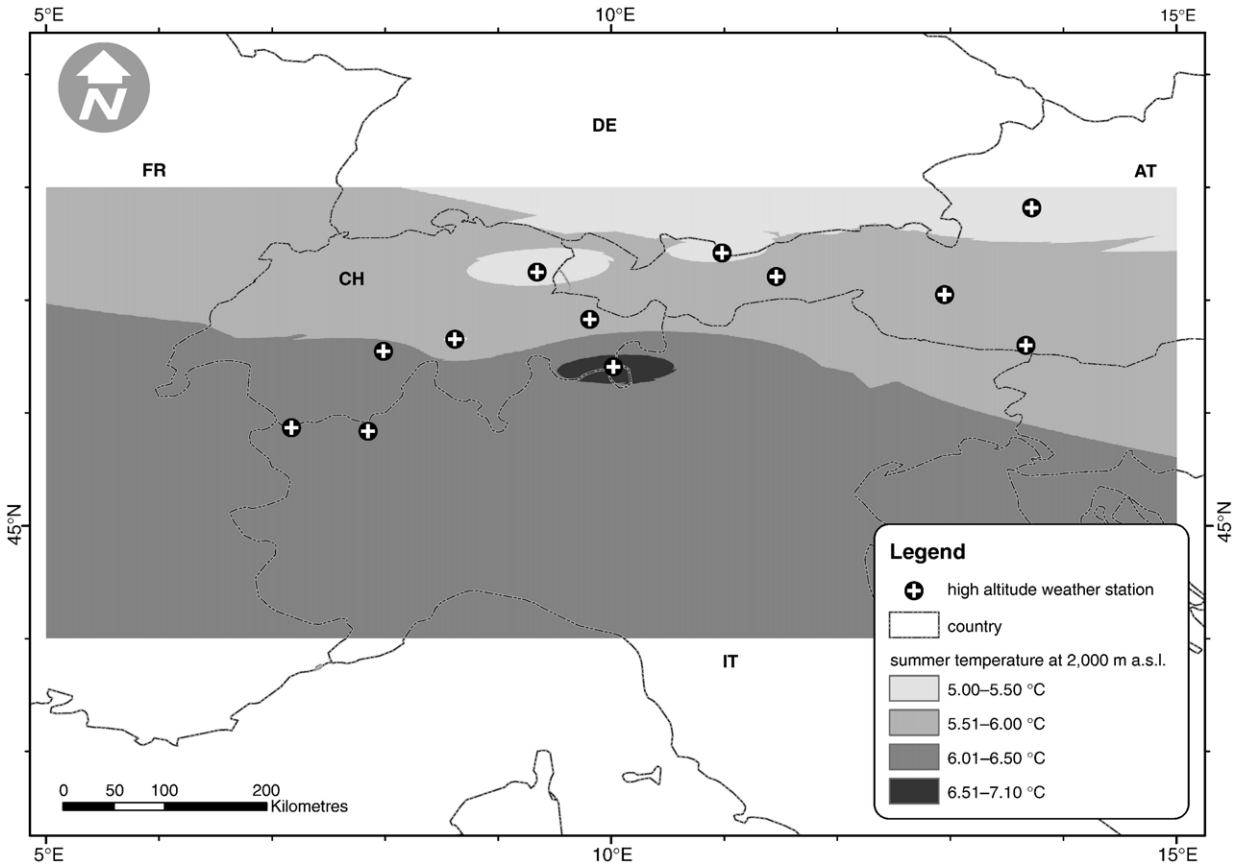

Fig. 3. The 6-month summer temperature field at 2000 m a.s.l. (1971–1990) as interpolated from 12 high altitude weather stations. A seasonal lapse rate of 0.67 °C per 100 m was used to altitude-adjust the seasonal mean temperature at weather stations to 2000 m a.s.l. The IDW (Watson and Philip, 1985) method was used for the interpolation.

2 km). Frei and Schär (1998) and Schwarb et al. (2001) calculated a regression between precipitation and altitude for each grid cell. Station data is weighted differently according to the extent to which they are representative of conditions at that grid cell. The weighting takes into account factors such as distance and difference in altitude from the grid cell, as well as varying aspect. However, in this study we find that the DEM that underlies the precipitation climatology differs significantly in altitude from the ELA_0, i.e., the altitude assigned to a grid cell in the precipitation climatology is significantly different from the measured ELA_0 (mean absolute difference of 161 m, with a maximum absolute difference of 655 m). Therefore, we use the precipitation–elevation gradients (ranging at ELA_0 locations from −2 to 78% per 100 m) to correct the precipitation of each grid cell in the glacier accumulation area to the corresponding ELA_0. Not knowing the exact location of the ELA_0 (only the location of the glacier boundaries and the altitude value of the ELA_0 are known) and of the uncertainties of the precipitation climatology, the precipitation at the ELA_0 is calculated as the mean of all precipitation grid cells covering the glacier accumulation area.

The variations in precipitation are complex and, in contrast to temperature variations, can be poorly correlated with altitude. Auer et al. (2005) show that the spatial mean decorrelation distances (R^2 decreasing below 0.5) of temperature (annual: 993 km, seasonal: 765 km, monthly: 722 km) are much larger than those of precipitation (annual: 149 km, seasonal: 120, monthly: 105 km). Hence, many fewer stations are needed to interpolate temperature at glacier locations. However, Oerlemans (2001, p. 37–38) demonstrates for the Morteratsch Glacier (Switzerland) that temperature at a nearby valley station may tend to become decoupled from the temperature measured at an automatic weather station located on the glacier surface (e.g., due to atmospheric inversions in the flat valley during winter), whereas the correlation with a high altitude weather station remains high. Therefore, we use temperature from 12 Alpine high altitude weather stations with continuous data series between 1971 and 1990, provided by MeteoSwiss,

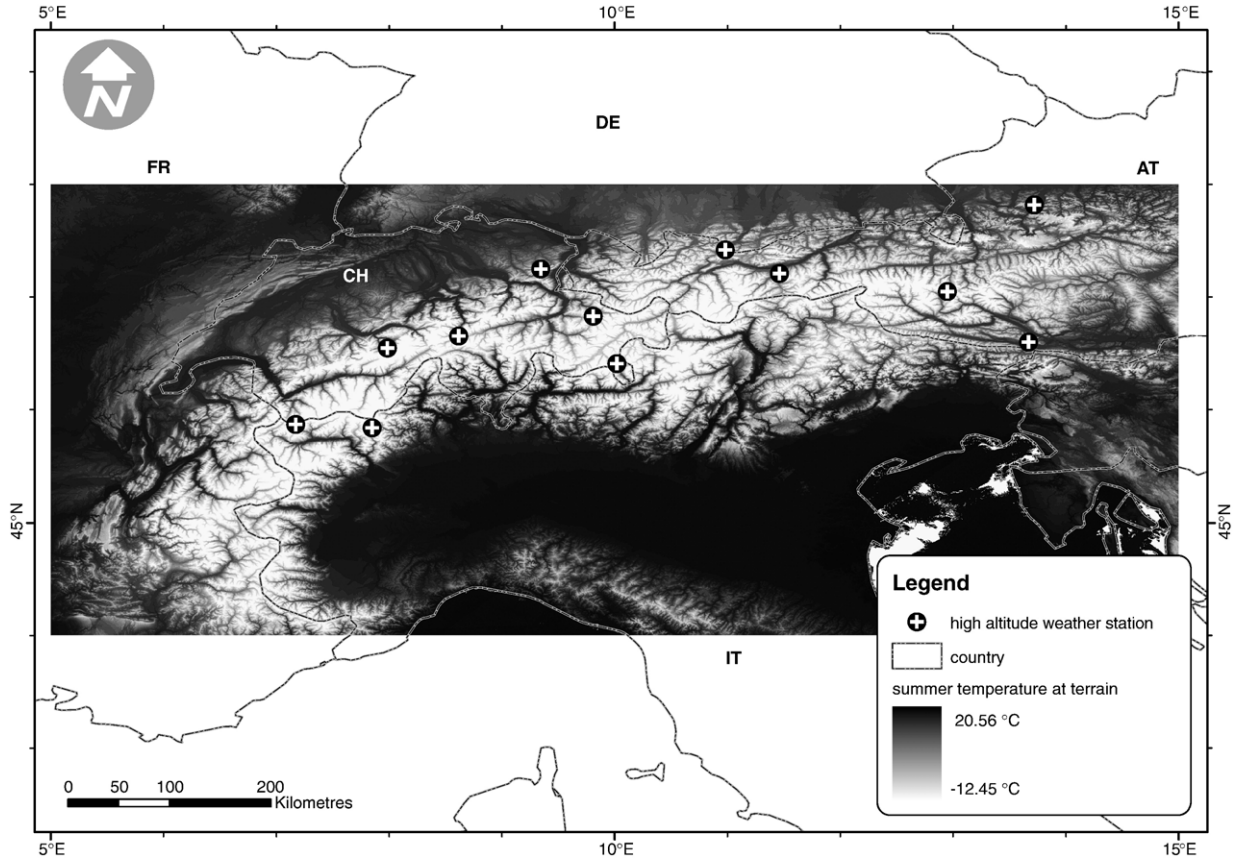

Fig. 4. The 6-month summer temperature on terrain (1971–1990). The data set was produced by extrapolating the temperature field at 2000 m a.s.l. (Fig. 3) to the altitude of the terrain (SRTM3, competed with SRTM30) using a seasonal lapse rate of 0.67 °C per 100 m.

Table 1
Precipitation and temperature at the ELA_0 for the period of 1971–1990. ELA_0 is calculated from the linear relationship between ELA and the specific net balance. Annual precipitation (P_a, sum) and 6-month winter precipitation (P_{O-M}, sum) are derived from the Alpine precipitation climatology by Frei and Schär (1998) and Schwarb et al. (2001). Annual temperature (T_a, average), 6-month summer temperature (T_{A-S}, average) and 3-month summer temperature (T_{JJA}, average) are interpolated at 2000 m a.s.l. from high altitude weather stations (see Fig. 1) and extrapolated to the ELA_0

Glacier name	Lat	Lon	ELA_0	P_a	P_{O-M}	T_a	T_{A-S}	T_{JJA}
	(°)	(°)	(m a.s.l.)	(mm)	(mm)	(°C)	(°C)	(°C)
Fontana Bianca (IT)	46.48	10.77	3177	1125	417	−5.43	−1.58	1.20
Gietro (CH)	46.00	7.38	3174	1250	604	−5.52	−1.63	1.21
Kesselwand (AT)	46.83	10.80	3106	1270	480	−5.19	−1.52	1.12
Careser (IT)	46.45	10.70	3088	1111	401	−4.86	−0.91	1.91
Vernagt (AT)	46.88	10.82	3076	1100	428	−5.03	−1.35	1.28
Gr. Aletsch (CH)	46.50	8.03	[a]2961	2926	1327	−4.18	−0.23	2.40
Hintereis (AT)	46.80	10.77	2933	1228	466	−4.13	−0.33	2.35
Rhone (CH)	46.62	8.40	2918	2031	1094	−4.04	−0.44	2.26
Gries (CH)	46.43	8.33	2852	2226	1036	−3.58	0.34	3.07
Plattalva (CH)	46.83	8.98	2772	1968	839	−3.14	0.64	3.34
Wurten (AT)	47.03	13.00	2770	2518	1063	−3.61	0.73	3.47
Silvretta (CH)	46.85	10.08	2755	1443	530	−2.93	0.89	3.56
Sonnblick (AT)	47.13	12.60	2731	2726	1135	−3.26	0.89	3.59
Limmern (CH)	46.82	8.98	2677	2012	857	−2.57	1.27	3.99

[a] The ELA_0 of Grosser Aletsch Glacier is calculated from mass balance data from the hydrological method, and ELA values interpolated from snow pits in the accumulation area of the glacier (Jungfraufirn) and aerial photographs.

Zurich, and the Central Institute for Meteorology and Geodynamics, Vienna. The 12 stations are all located above 2000 m a.s.l., with the exception of Feuerkogel (Austria) at 1618 m a.s.l. Monthly lapse rates are empirically derived from temperature and elevation values of the 12 stations. All of these linear regression analyses show high correlations (R^2 above 0.9) and range from 0.54 °C per 100 m in December to 0.71 °C per 100 m in July. Seasonal mean temperatures and lapse rates are calculated. With these empirically derived lapse rates, seasonal temperatures are altitude-adjusted to 2000 m a.s.l. Using the inverse distance weighted (IDW; Watson and Philip, 1985) interpolation method, temperatures are interpolated over the entire Alps. Anisotropy is taken into account by specifying a lower power along and a higher power against the Alpine ridge (specifying a lower value for power will provide more influence to surrounding points farther away). Fig. 3 shows the altitude-adjusted 6-month summer temperature field at 2000 m a.s.l. over the greater Alpine region. Temperature ranges from 5.0–7.1 °C. At glacier locations the empirical lapse rates are used again to extrapolate temperatures at 2000 m a.s.l. to the ELA_0. The same principle is applied to produce an Alpine-wide data set of temperature on terrain, with a resolution of 3 arc sec (approx. 100 m), by extrapolating the temperature field at 2000 m a.s.l. with the seasonal lapse rate to the altitude of a DEM (Fig. 4). As already mentioned, the exact location of the ELA_0 is not known and it might also differ from the elevation of the corresponding grid cell of the DEM. For the estimation of temperature and precipitation at the ELA_0, used to derive the empirical relationship, we consider, therefore, the ELA_0 instead of the corresponding altitude of the DEM. Hence, temperature and precipitation values at the location of the mass balance observations might differ from the values at the corresponding locations in the gridded precipitation and temperature climatologies.

Annual and 6-month winter precipitation, and annual and 6- and 3-month summer temperatures at the ELA_0

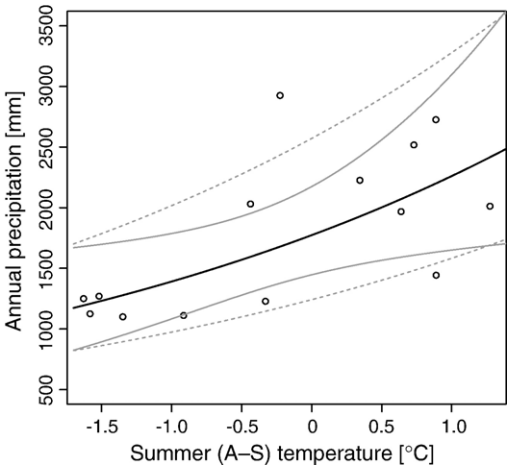

Fig. 5. Annual precipitation and 6-month summer temperature at the ELA_0 for the period 1971–1990 (cf. Table 1). The exponential regression model (Eq. (1); black line) performs with a R^2 of 0.49. The boundaries of the 95% confidence interval (Eq. (2); grey line) are conservatively approximated by shifting the regression model (Eqs. (3) and (4); dashed grey lines).

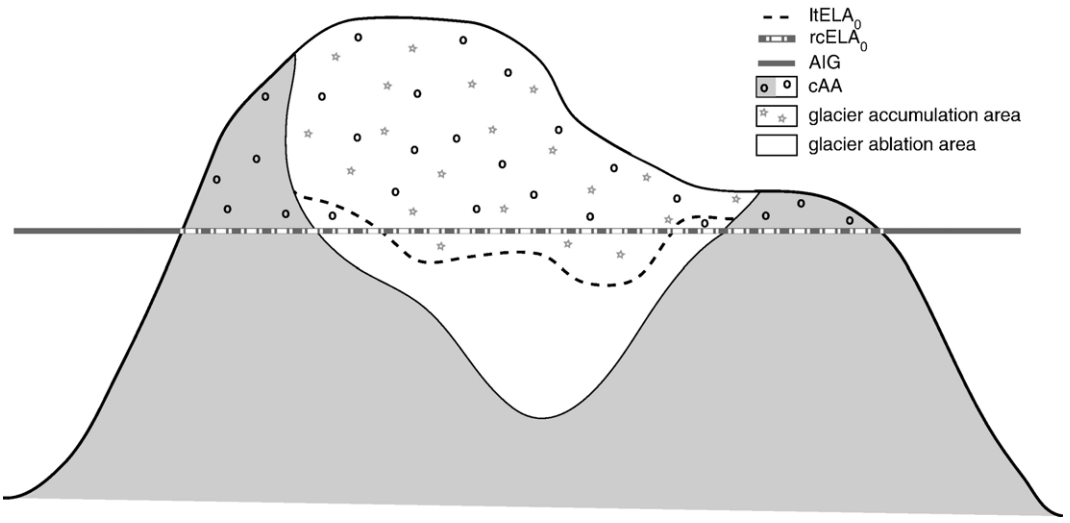

Fig. 6. Diagram to explain the concept of the AIG and its association with $ltELA_0$, $rcELA_0$ and cAA. Figure modified after Lie et al. (2003a).

of the 14 Alpine glaciers are shown in Table 1. The empirical relationship between annual precipitation (P_a) and the 6-month summer temperature (T_{A-S}) at the ELA_0 performs best with an R^2 of 0.49 on a 1% significance level (p-value of 0.0052) and can be expressed by the regression equation:

$$P_a = 1773 \cdot e^{0.2429 \cdot T_{A-S}} \quad (1)$$

Eq. (1) is plotted in Fig. 5 together with the upper and lower boundaries of the 95% confidence interval which can be formulated as:

$$P_a = 1773 \cdot e^{0.2429 \cdot T_{A-S}^{\pm 0.1985 \cdot \sqrt{(1+(T_{A-S}+0.2301)^2}}} \quad (2)$$

These boundaries describe the possible range of annual precipitation, at a 5% significance level, for a given 6-month summer temperature at the ELA_0.

The 95% confidence interval boundaries can be approximated by a shift of Eq. (1) in such a manner that the new equations for the lower boundary, Eq. (3), and upper boundary, Eq. (4), describe a confidence interval greater than 95% within the temperature data range and lower than 95% outside the temperature data range, respectively.

$$P_a = 0.7 \cdot 1773 \cdot e^{0.2429 \cdot T_{A-S}} \quad (3)$$

$$P_a = 1.45 \cdot 1773 \cdot e^{0.2429 \cdot T_{A-S}} \quad (4)$$

3.2. Distributed modelling of the regional climatic ELA_0

To apply Eq. (1) in space, we implement the approach from Lie et al. (2003a). Along with this, we introduce temperature lapse rate and precipitation–elevation gradient to derive temperature and precipitation at the AIG. Temperature at the AIG (T_{AIG}) can be derived from the temperature at a known altitude (T_0), the lapse rate (ΔT) in degrees Celsius per 100 m and the height of the AIG above the terrain (h, in 100 m units):

$$T_{AIG} = T_0 - (\Delta T \cdot h) \quad (5)$$

The precipitation at the AIG (P_{AIG}) can be derived from the precipitation at a known altitude (P_0), the precipitation–elevation gradient (ΔP) in percent per 100 m and the height of the AIG above the terrain (h, in 100 m units):

$$P_{AIG} = P_0 \cdot (1 + \Delta P)^h \quad (6)$$

By combining Eqs. (5) and (6) with Eq. (1), the expression becomes:

$$P_0 \cdot (1 + \Delta P)^h = 1773 \cdot e^{0.2429 \cdot (T_0 - (\Delta T \cdot h))} \quad (7)$$

Solving Eq. (7) with respect to the only unknown parameter h, the AIG is:

$$AIG = ALT_{DEM} + (h \cdot 100) = ALT_{DEM} + \left(\frac{\ln(1773) + 0.2429 \cdot T_0 - \ln(P_0)}{\ln(1 + \Delta P) + 0.2429 \cdot \Delta T} \cdot 100 \right) \quad (8)$$

where ALT_{DEM} is the altitude of the terrain. The $rcELA_0$ can now be computed from the intersection of the DEM with the AIG, where ALT_{DEM} is equal to AIG (or: $h = 0$).

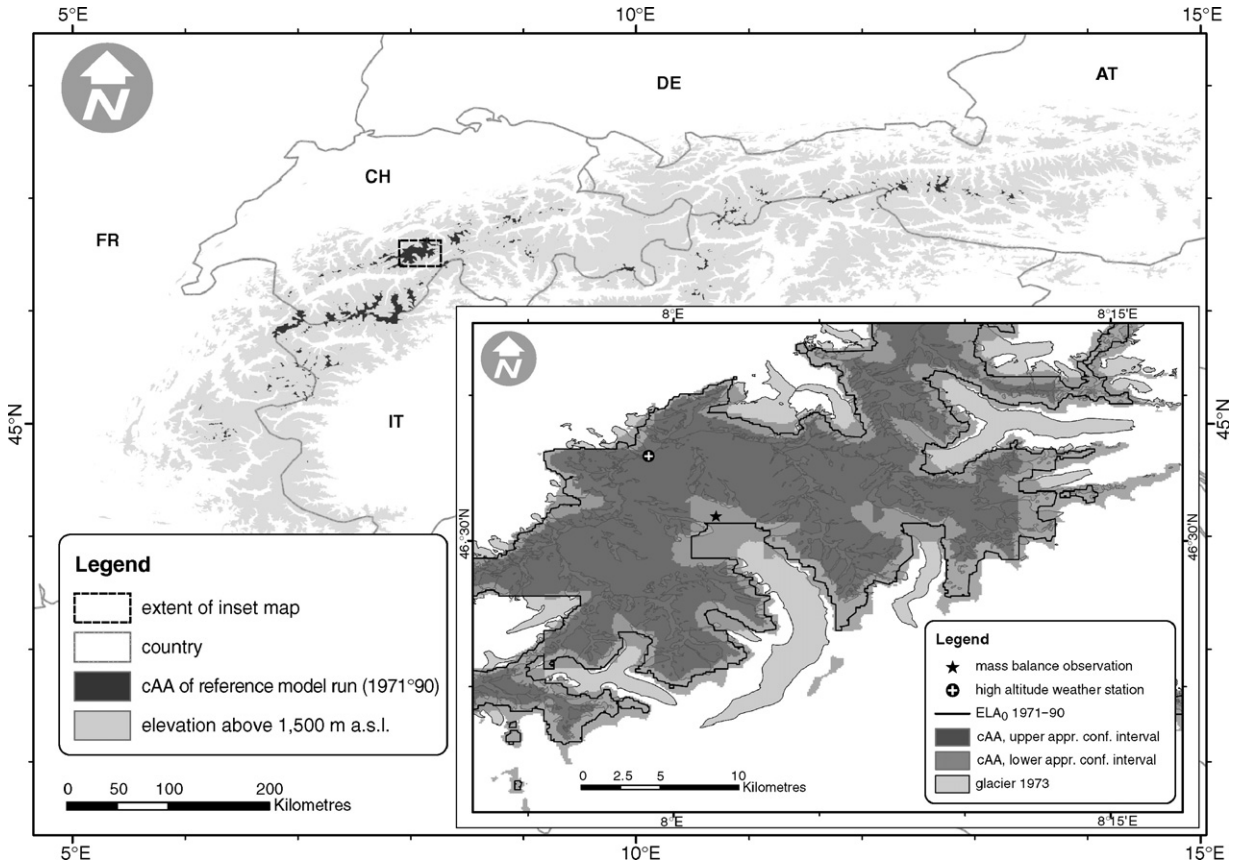

Fig. 7. cAA of the reference model run (1971–1990). The inset map shows the ELA_0 of the reference model run (black line) and the cAAs of the corresponding lower (grey) and upper (dark grey) boundaries of the approximated confidence interval. Glacier extents of 1973 from the Swiss Glacier Inventory are shown in light grey.

The climatic accumulation area (cAA) corresponds to the regions where the ALT_{DEM} is above the AIG (or: $h<0$):

$$\mathrm{AIG}\begin{cases} < & \mathrm{ALT_{DEM}} & \rightarrow & \mathrm{cAA} \\ = & \mathrm{ALT_{DEM}} & \rightarrow & \mathrm{rcELA_0} \\ > & \mathrm{ALT_{DEM}} & \rightarrow & \mathrm{no.cAA} \end{cases} \quad (9)$$

A schematic representation of the AIG and its association with $ltELA_0$, $rcELA_0$ and cAA appears in Fig. 6.

The AIG, $rcELA_0$ and cAA are modelled in space using the annual precipitation data (in mm) and the corresponding annual precipitation–elevation gradients (in percent per 100 m) from Frei and Schär (1998) and Schwarb et al. (2001) and 6-month summer lapse rate (0.67 °C per 100 m) and 6-month summer temperature on terrain as input raster data sets. The summer temperature data set is extrapolated with the summer lapse rate from the altitude-adjusted temperature field at 2000 m a.s.l. (Fig. 3) to the altitude of the DEM (Fig. 4). The latter is the 3 arc sec version created by the Shuttle Radar Topography Mission (SRTM3; spatial coverage from 61° N to 57° S) and resampled to 100 m spatial resolution for our purposes. The data can be downloaded for free from a NASA ftp-server (ftp://e0mss21u.ecs.nasa.gov/srtm/) and are described in Rabus et al. (2003). Larger gaps in the SRTM3 data set have been filled by resampled 30 arc sec SRTM30 elevation data, and can be obtained from the

Table 2
Overview of the seven model runs. Deviations in temperature and precipitation of the six sensitivity runs from the reference model run ($MR_{1971-1990}$)

	MR	MR	MR	MR	MR	MR	MR
	1971–1990	T+1	T−1	P+25	P−25	T−0.6	T+3/ P+10
ΔT [°C]	0	+1	−1	0	0	−0.6	+3
ΔP [%]	0	0	0	+25	−25	0	+10

same source. The distributed modelling is implemented and automated using the ESRI software ArcGIS 9.0. A model run takes a few minutes of computing time.

In Fig. 7 the modelled cAA is shown for the reference period 1971–1990, and the maximum spatial extent of the investigation area (6–14° E, 44–48° N) is defined by the data set with the minimum spatial extent (precipitation data). By combining Eqs. (5) and (6) with Eqs. (3) and (4), AIG, rcELA$_0$ and cAA of the boundaries of the approximated confidence interval can be applied in space as well (Fig. 7, inset map).

3.3. Sensitivity study

In addition to the model run for the reference period 1971–1990, six more model runs were carried out to study the sensitivity of the ELA$_0$ to changes in temperature and precipitation. Temperature and/or precipitation are altered by a uniform deviation over the entire investigation area (i.e., the entire gridded climatologies). Table 2 gives an overview on the seven model runs.

MR$_{T+1}$ and MR$_{T-1}$ as well as MR$_{P+25}$ and MR$_{P-25}$ are sensitivity studies with deviations only in temperature or

Table 3
Basin mean ELA$_0$ of the reference model run (MR$_{1971-1990}$) and ELA$_0$ deviations of the six sensitivity runs. Zonal borders come from the HYDRO1k DEM (http://LPDAAC.usgs.gov). In addition, zonal means within the 1973 outlines of the Swiss Glacier Inventory (Kääb et al., 2002; Paul et al., 2002) for glaciers larger than 1 km^2 are given

Hydrological basin (no.)	MR$_{1971-1990}$ (m a.s.l.)	MR$_{T+1}$ (m)	MR$_{T-1}$ (m)	MR$_{P+25}$ (m)	MR$_{P-25}$ (m)	MR$_{T-0.6}$ (m)	MR$_{T+3/P+10}$ (m)
Lech (6985)	#	#	*	*	#	*	#
Isar (6988)	2592	+190	−137	−130	#	−60	#
Enns (7078)	2772	+131	−124	−110	+148	−78	+319
Traun (7080)	#	#	*	*	#	*	#
Linth (7124)	2784	+135	−134	−125	+149	−80	+340
Reuss (7130)	2784	+154	−131	−124	+167	−82	+366
Mur (7171)	2716	+130	−47	−47	+130	+18	#
Inn (7188)	3102	+118	−154	−142	+152	−95	+375
Aare (7194)	2795	+137	−125	−117	+150	−72	+310
Ill (7196)	#	#	*	*	#	#	#
Landquart (7210)	2807	+119	−80	−73	+113	−32	#
Ziller (7211)	2873	+150	−128	−121	+174	−83	+359
Arve (7237)	2895	+141	−120	−112	+170	−64	+360
Rhone (7246)	2966	+130	−132	−122	+147	−73	+315
Hinterrhein (7250)	2805	+126	−116	−103	+144	−71	+302
Drau (7261)	2810	+118	−96	−86	+145	−62	+309
Adige (7268)	3110	+135	−128	−114	+151	−80	+296
Vorderrhein (7272)	2896	+163	−44	−42	+168	−24	+327
Toce (7303)	2878	+161	−145	−134	+192	−92	+414
Adda (7332)	3144	+121	−194	−188	+171	−116	+351
Piave (7356)	2981	#	−83	−62	#	−66	#
Isere (7403)	3154	+131	−154	−142	+166	−90	+368
Aosta (7411)	3001	+112	−118	−107	+124	−65	+283
Drava (7420)	#	#	*	*	#	*	#
Chiese (7427)	3079	+137	−119	−110	+184	−91	#
F. Sesia (7438)	2980	+116	−117	−104	+113	−66	+295
Oreo (7487)	3159	+138	−135	−134	+165	−82	+325
D. Riparia (7538)	3144	+114	−138	−130	+190	−78	#
Durance (7557)	3183	+127	−193	−166	+169	−116	+344
Chisone (7581)	3148	+184	−83	−79	+184	−91	+368
Po basin (7605)	2987	#	−123	−108	#	−76	#
Po fount (7673)	#	#	*	*	#	*	#
Var (7737)	3077	#	−201	−172	#	−131	#
Argens (7741)	#	#	*	#	#	#	#
Liguria (7747)	#	#	*	*	#	*	#
All hydro basins	2951	+137	−125	−114	+157	−75	+336
Swiss glaciers	2946	+126	−118	−107	+140	−65	+308

* The calculation of an rcELA$_0$ difference from the reference run is not possible, since for one model run the #AIG is above the highest peaks in of the corresponding hydrological basin.

precipitation. $MR_{T-0.6}$ represents a summer temperature cooling of 0.6 °C, as assumed by Maisch et al. (2000) for the year 1850. $MR_{T+3/P+10}$ applies a warming of the summer temperature of 3 °C and a concurrent rise in precipitation by 10%. This corresponds to a moderate climate change scenario as published by OcCC (2004), commissioned by the Swiss Federal Office of Energy (SFOE). This study is based on IPCC (2001) and estimates a summer (JJA) temperature rise of 0.8–5.1 °C by 2050 for the northern and 1.0–5.6 °C for the southern slope of the Swiss Alps, respectively. It estimates precipitation to decrease in summer and increase in winter. For winter (DJF) precipitation a rise of 5–23% is indicated by 2050.

Reference and sensitivity model runs are analysed for individual glacier regions, within the hydrological basins, as derived from the HYDRO1k DEM (provided by the Land Processes Distributed Active Archive Centre located at the U.S. Geological Survey's EROS Data Centre: http://LPDAAC.usgs.gov), and within the 1973 outlines of the Swiss Glacier Inventory (Kääb et al., 2002; Paul et al., 2002) for glaciers larger than 1 km^2.

4. Results

4.1. Empirical relationship between precipitation and temperature at the ELA_0

Precipitation at the glacier ELA_0 (Eq. (1), Table 1) shows a non-linear increase with increasing temperature. The differences in R^2 between the applied exponential trends and linear trends range from 0.06–0.08, i.e., 6–8% of the explained variance. The empirical relationships with annual precipitation perform better than the ones with 6-month winter precipitation, with R^2 differences of 0.10–0.12. For the distributed modelling of the AIG, the $rcELA_0$ and the cAA the relationship between annual precipitation and 6-month summer temperature is used (Eq. (1)), as it performs best with an R^2 of 0.49 on a 1% significance level (p-value of 0.0052).

4.2. Modelled glacierisation of the reference run (1971–1990)

The AIG of the reference model run (1971–1990), shows two culminations with AIG values above 3100 m a.s.l.; one ranging from the southern Valaisan Alps, Switzerland, to the south-western Alps and another one between the Rhaetian Alps, Switzerland, over the South Tyrol, Italy, to the Upper Tauern, Austria. There is an AIG depression over the Ticino Alps, Switzerland, and a generally lower AIG on the northern Alpine slope.

Table 3 lists the $rcELA_0$ averaged within the hydrological basins and within the Swiss glacier outlines. As the $rcELA_0$ represents the intersection of the AIG with the DEM, it reproduces the general image of the AIG. It ranges from 2591 m a.s.l. (Isar) to 3183 m a.s.l. (Durance) with a mean value of 2951 m a.s.l. However, some hydrological basins show an average, caused by local topographic effects, that does not correspond to the $rcELA_0$ of the sub-regions. The most pronounced example is the Rhone basin in the Valais, Switzerland. It has an average ELA_0 of 2966 m a.s.l. with a standard deviation of 161 m. This is produced by $rcELA_0$ values below 2800 m a.s.l. in the northern Valais and above 3100 m a.s.l. in the southern Valais.

Over the entire Alps the cAA covers an area of 3059 km^2. As the cAA is simply the terrain above the $rcELA_0$, it does not distinguish between glacier surface and ice-free rock walls. In a first order approach this can be taken into account by applying a slope-dependent glacier fraction to the modelled cAA. Table 4 shows the slope-area distribution (derived from the SRTM3) within the cAA and within the parts of the 1973 outlines of the Swiss Glacier Inventory inside the cAA of a test area (Canton Valais, Switzerland, corresponding approximately to the Rhone basin). From these parameters, glacier fractions are calculated for the nine slope classes and applied to the slope-area distribution of the Alpine cAA. These empirical glacier fractions are dependent on quality and resolution of the DEM used and therefore have to be re-evaluated when using other DEMs. The corrected cAA equals 1950 km^2 and corresponds to an AAR_0 of 0.67 of the measured total Alpine glacier area in the 1970s, which was 2909 km^2 (Zemp et al., in press).

4.3. Model validation

The model error can be described by the deviations of the modelled AIG values of the 14 glaciers from the measured ELA_0. The mean absolute difference is 66.7 m with a standard deviation of 55.4 m. The greatest deviations are found for Silvretta Glacier, where the measured ELA_0 is 214 m below the modelled AIG, and for Grosser Aletsch Glacier, where the ELA_0 is 127 m above the AIG. To get an estimation of the possible deviation of the $ltELA_0$ from the $rcELA_0$ (as modelled), Eq. (1) is substituted by the two approximations of the confidence interval boundaries, Eqs. (3) and (4), to calculate a spatial confidence zone. This results in average deviations of −177 m and +209 m from the reference $rcELA_0$, based on Eq. (1).

The resulting cAA is checked in a qualitative manner by comparison with the outlines from the 1973 Swiss

Table 4
Slope-area distribution (in km^2) within the cAA (1971–1990) and within the 1973 outlines of the Swiss Glacier Inventory inside the cAA (1971–1990), computed in the Canton Valais, Switzerland (corresponding approximately to the Rhone basin). The glacier fraction of each slope class (in %) is calculated based on this distribution

Data set	0–10°	11–20°	21–30°	31–40°	41–50°	51–60°	61–70°	71–80°	81–90°
cAA	220.0	370.7	290.3	171.7	70.8	13.4	1.5	<0.1	0
Glacier area within cAA	196.3	288.7	169.8	67.7	22.8	3.8	0.4	0	0
Glacier fraction	89	78	58	39	32	29	29	0	0

Glacier Inventory and with LandsatTM images dating from the 1990s. The modelled cAA corresponds well overall to the real accumulation areas of Alpine glaciers and there are minor quantities of cAA cells in regions with no glacierisation. A general overestimation of the accumulation areas on SE–SW slopes and underestimation on NE–NW slopes can be found.

4.4. Sensitivity study

The rcELA$_0$ deviations of the sensitivity model runs from the reference run (1971–1990) within the hydrological basins are shown in Table 3. A temperature change of ±1 °C leads to an average rcELA$_0$ deviation of +137/−125 m, ranging from +112 m (Aosta) to +190 m (Isar) and from −44 m (Vorderrhein) to −201 m (Var), respectively. A precipitation change of ±25% leads to an average rcELA$_0$ deviation of −114/+157 m, with a range similar to the 1° temperature deviation. MR$_{T-0.6}$ results in an average rcELA$_0$-decrease of 75 m, ranging from 24 m to 131 m. The increase of 18 m within the Mur basin is an undesired side-effect caused by the very small number of cAA cells. The occurrence of an additional glacierised peak in the MR$_{T-0.6}$ run leads to an average

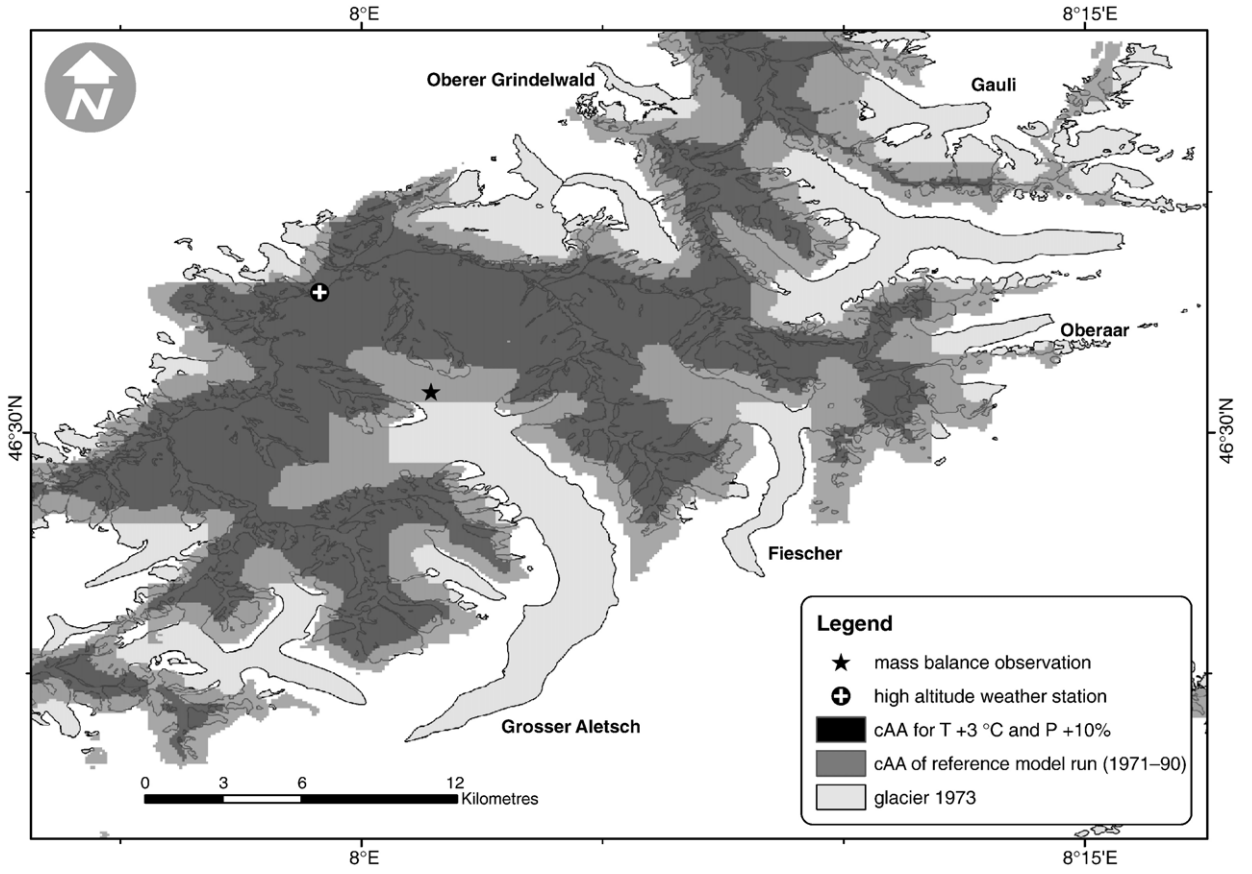

Fig. 8. cAA of the reference model run (1971–1990, grey) and cAA of the MR$_{T+3/P+10}$ (dark grey) in the region of Grosser Aletsch glacier, Switzerland. Glacier extents in 1973 from the Swiss Glacier Inventory are shown in light grey.

rcELA$_0$ higher than the one from the reference model run (1971–1990). The total cAA of the MR$_{T-0.6}$ run amounts to 4157 km^2. MR$_{T+3/P+10}$ leads to an average rcELA$_0$ rise of 336 m and the disappearance of glaciers in eight out of 28 basins. The corresponding total cAA over the entire Alps shrinks to 812 km^2. When the slope-dependent glacier fraction (Table 4) is applied, the cAA of the MR$_{T-0.6}$ and the MR$_{T+3/P+10}$ amounts to 2650 km^2 and 504 km^2, respectively. The average rcELA$_0$ and the deviations corresponding to the sensitivity runs, calculated within the 213 Swiss glacier outlines, represent a rcELA$_0$ subset of the hydrological basins Aare, Adda, Hinterrhein, Inn, Landquart, Linth, Reuss, Rhone, Toce and Vorderrhein. The deviations within the glacier outlines are slightly more moderate than those of the corresponding basin. The MR$_{T-0.6}$ induced a rcELA$_0$ lowering of 65 m.

Fig. 8 and 9 show the modelled cAA of the reference run (1971–1990) and of MR$_{T+3/P+10}$ for the regions of Grosser Aletsch Glacier and Rhone Glacier. To facilitate a qualitative check, the outlines of the 1973 Swiss Glacier Inventory are shown as well. The modelled cAA of the reference run (1971–1990) covers the accumulation areas of the Swiss glacier outlines of 1973 reasonably well. In flat areas (e.g., upper tongue of Grosser Aletsch Glacier, Fig. 8) the coarser resolved precipitation data may determine the rcELA$_0$ (i.e., long, sharp boundaries), whereas on steeper terrain, the temperature data set with higher resolution (20 times) is the determining factor. In general, cAA is overestimated on SE–SW slopes and underestimated on NE–NW slopes. The rcELA$_0$ rise between the reference run and MR$_{T+3/P+10}$ leads to a much more pronounced cAA reduction in flat regions compared to steep slopes.

In regions where the glacier outlines are available, the rise of the rcELA$_0$ can be derived for individual glaciers. In Fig. 8, the rise of the rcELA$_0$ between the two model runs amounts to 249 m for Grosser Aletsch Glacier, 315 m for Fiescher Glacier, 314 m for Oberaar Glacier, 310 m for Gauli Glacier and 353 m for the Oberer

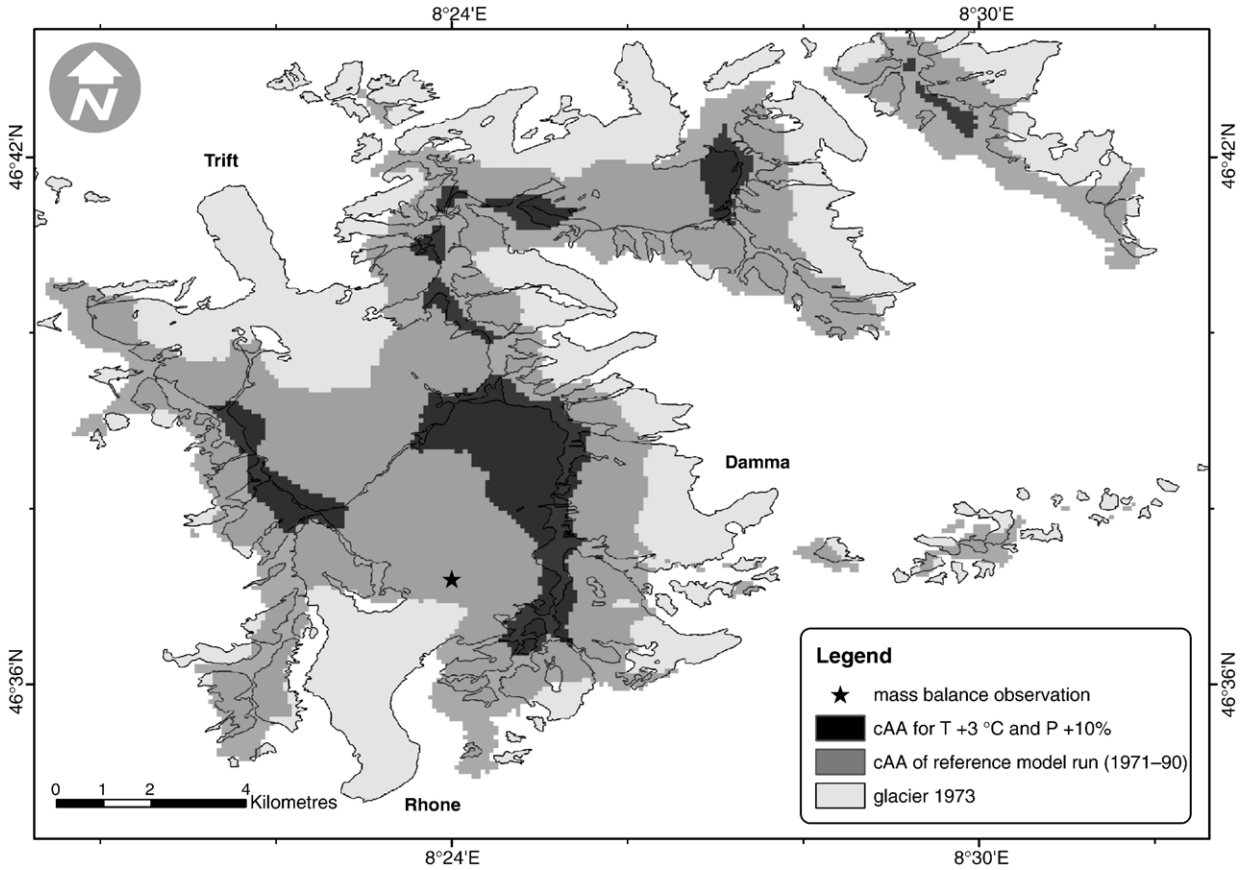

Fig. 9. cAA of the reference model run (1971–1990, grey) and cAA of the MR$_{T+3/P+10}$ (dark grey) in the region of Rhone glacier, Switzerland. Glacier extents in 1973 from the Swiss Glacier Inventory are shown in light grey.

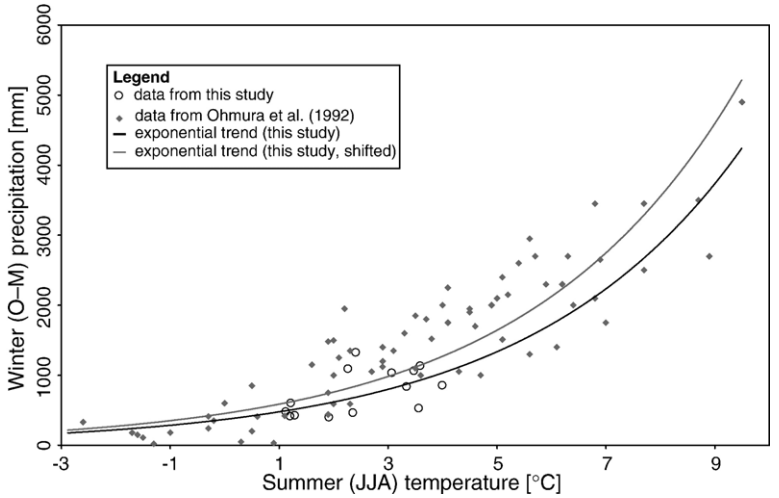

Fig. 10. The 6-month winter precipitation and the 3-month summer temperature at the ELA_0. Comparison between the data set presented in this study (black circles) and the one by Ohmura et al. (1992; grey diamonds). The exponential model (black line) based on the 12 data points from this study is shown together with a shifted exponential curve assuming a systematic precipitation measurement error of 23% (grey line).

Grindelwald Glacier. In Fig. 9 the $rcELA_0$ rises by 384 m at Rhone Glacier, 381 m at Damma Glacier and 374 m at Trift Glacier. In this region the temperature rise of the $MR_{T+3/P+10}$ leads to a strong reduction and disintegration of the cAA.

5. Discussion

5.1. Error estimations and model uncertainties

The 14 glaciers, on which the relationship between precipitation and temperature at the ELA_0 is based, are geographically and climatologically well-distributed over the Alps. Only the south-western Alps between France and Italy lack temperature and mass balance data. In this region, temperature measurements from high altitude weather stations began only after 1990. Mass balance data from Saint Sorlin (45° 11′ N, 6° 10′ E) and Sarennes (45° 7′ N, 6° 10′ E) exist, but ELA values are not available.

The precipitation data set by Frei and Schär (1998) and Schwarb et al. (2001) is based on more than 6000 data points and is currently the best available data set at this resolution covering the entire Alps. The applied interpolation method takes into account the fact that the precipitation–elevation gradients can vary considerably from one region to another (Schwarb et al., 2001). Approaches using a constant precipitation–elevation gradient for the precipitation extrapolation to the ELA may work in regions dominated by orographic precipitation due to frontal cyclones flowing perpendicular to the orientation of the mountain ridge (e.g., western side of the Canadian Rockies, western mountains in southern Norway), but will not include the effects of the complex gradient-patterns of the European Alps. However, in the precipitation climatology used, the data are not adjusted to the systematic precipitation measurement error, since the data needed to do this (wind, aspect of the station) are not available. Sevruk (1985) estimates this error for mean annual precipitation at 15–30% above 1500 m a.s.l. Hence, Eq. (1) has to be adapted if it is applied or compared to precipitation data with corrected systematic measurement error.

As already mentioned in Section 3: Methods, the spatial decorrelation distance is much greater for temperature than for precipitation. Together with the high coefficients of determination ($R^2 > 0.9$) of the derived temperature lapse rates, this justifies the interpolation of the general high altitude temperature field (at 2000 m a.s.l.) over the Alps based on the data from only 12 stations. Comparisons of the applied IDW interpolation method (considering anisotropy) with IDW (not considering anisotropy) and KRIGING (Oliver and Webster, 1990) show a mean temperature difference of 0.04 °C (with a standard deviation of 0.16 °C) and −0.03 °C (with a standard deviation of 0.35°), respectively. Assuming a temperature lapse rate of 0.67 °C per 100 m this corresponds to a mean ELA difference of about 5 m. In a test area of about 42 km × 34 km in the southern Valaisan Alps, Switzerland, comparisons of the SRTM3 (used to extrapolate temperature at 2000 m a.s.l. to the terrain) with the

DEM25L2 (a high-quality Swiss DEM with a resolution of 25 m) show a mean altitude difference between the two DEMs of 7.7 m with a standard deviation of 53.7 m. In the regions where the SRTM3 gaps had to be filled with the SRTM30, the DEM difference amounts to 100 m with a standard deviation of 158 m. This shows that the temperature error due to the applied interpolation method is of the same order of magnitude as the one due to errors in the DEM. However, in the presented distributed model the step from a non-cAA grid cell to a cAA grid cell is dominated by the parameter with the greatest variability from one cell to its immediate neighbours. The mean absolute difference from a grid cell to its eight neighbours of the used DEM is 15.9 m, whereas that of temperature at 2000 m a.s.l. is 0.0003 °C (corresponding to 0.04 m). This means that the altitude of the terrain is the decisive factor determining in the spatial distribution of the $rcELA_0$, superimposed by the precipitation field and the temperature field at 2000 m a.s.l. over the Alps.

The non-linearity of the empirical relationship between precipitation and temperature at the ELA_0, Eq. (1), is physically sound since, with increasing temperature, the rise of the ELA leads to a longer ablation season. Hence the influence of the temperature lapse rate becomes more dominant and the mass balance gradient increases. An additional amount of solid precipitation is needed to compensate the melting. Eq. (1) includes an uncertainty of about 500 mm precipitation for a given temperature at the ELA_0. The corresponding confidence zone is a conservative approximation of the 95% confidence interval (Eq. (2), Fig. 5). By applying this confidence zone in space, an uncertainty buffer with an average deviation of about ±190 m from the $rcELA_0$ of the reference run can be modelled, that accounts for measurement errors and for deviations of the $ltELA_0$ from the modelled $rcELA_0$ due to influences not included in the model (e.g., snow drift, avalanches, solar radiation). The general overestimation of the cAA on SE–SW slopes and underestimation on NE–NW slopes can be interpreted as differences, for example in solar radiation. Distributed mass balance models are needed (e.g., Klok and Oerlemans, 2002; Paul et al., in press) in order to account for these topographic effects. The influence of the uncertainty in $rcELA_0$ on the cAA is indirectly proportional to the slope of the terrain, i.e., the steeper the terrain, the smaller the corresponding error of the cAA.

Beyond the range of precipitation and temperature values, used for the derivation of Eq. (1) the uncertainties increase non-linearly. However, a comparison with worldwide data from Ohmura et al. (1992) shows that the empirical relationship derived from the 14 Alpine glaciers is also plausible for strongly continental and strongly maritime regions in the world. In Fig. 10, the 3-month summer temperature and the 6-month winter precipitation at the ELA_0 are plotted for the 14 Alpine glaciers in this study as well as for 69 glaciers worldwide as published in Ohmura et al. (1992). In addition, the exponential relationship derived only from the 14 Alpine glaciers is drawn, together with a shifted exponential curve that assumes a systematic precipitation measurement error of 23% (i.e., mean of the estimated measurement error of 15–30% for altitudes above 1500 m a.s.l.; Sevruk, 1985). We have not combined these two data sets in order to derive a worldwide valid relationship between precipitation and temperature at the ELA_0, as they are not based on the same methodology, and in particular because the precipitation figures for Alpine glaciers existing in both data sets differ significantly. However, it is a future aim to extend the range of validity of the relationship, towards both more continental and more maritime regions. We recommend the determination of monthly, seasonal or at least annual precipitation and temperature at the ELA_0 of all glaciers with mass balance measurements. The determination of these two parameters together with the calculation of the ELA should become a standard for mass balance measurements.

The qualitative check of the cAA with the 1973 Swiss Glacier Inventory and with LandsatTM images dating from the 1990s, as well as the resulting AAR of 0.67 (calculated from the modelled cAA and the measured glacier area of the 1970s), confirm the overall accuracy of the modelled $rcELA_0$ and cAA. This can be quantitatively validated using a classification error matrix (Lillesand and Kiefer, 1994: 612–618) as soon as glacier outlines for the entire Alps are available and the real Alpine AAR value(s) are known. In addition, distributed mass balance values can be used to quantify the deviations of the $ltELA_0$ from the $rcELA_0$.

5.2. Findings from the distributed modelling in comparison with other studies

For the first time, $rcELA_0$ and cAA have been modelled at reasonable spatial resolution over the entire European Alps. Qualitative comparisons show that the modelled cAA of the reference model run (1971–1990) corresponds well overall to the real accumulation areas of Alpine glaciers. The cAA is clearly underestimated only between the Silvretta group and the Bernina group, in the eastern part of Switzerland, or only exists when the lower

confidence boundary, Eq. (3), is used instead of the reference run, based on Eq. (1). In this region, the AIG is above many peaks, i.e. there is no cAA. The reason for this is found in the underestimation of the precipitation in that region. To decrease the AIG at the location of Silvretta Glacier to the terrain (so that the AIG becomes a $rcELA_0$), an increase in annual precipitation of 757 mm (+53%) would be needed. To sustain a glacier at that location another decrease in the $rcELA_0$ by 200 m is required, which would result in a total precipitation increase of about 1800 mm (+125%). The probable cause of the underestimation of precipitation in the Silvretta region is the climatology by Frei and Schär (1998) and Schwarb et al. (2001). This is also supported by the fact that the Hydrological Atlas of Austria (2003) differs in this part by about 1600 mm from the precipitation climatology by Frei and Schär (1998) and Schwarb et al. (2001).

The sensitivity model runs show that a temperature change of ± 1 °C would be compensated by a precipitation increase/decrease of 25%. The relative precipitation change corresponds to a mean absolute change over the greater Alpine region of about 300 mm. This is in agreement with Oerlemans (2001) and Braithwaite and Zhang (2000), who showed from mass balance modelling that a 25% increase in annual precipitation is typically needed to compensate for the mass loss due to a uniform warming of 1 °C. Kuhn (1981) calculated a rise of the ELA by 100 m if either the winter accumulation decreases by 400 mm or if the summer free air temperature increases by 0.8 °C. $MR_{T-0.6}$ leads to an average ELA_0-decrease of 75 m over the entire Alps and of 65 m within the 1973 outlines of the Swiss Glacier Inventory larger than 1 km^2. This corresponds well to the reconstructed ELA rise of 69 m between 1850 and 1973 presented by Maisch et al. (2000). The cAA difference of −26% between $MR_{T-0.6}$ and $MR_{1971-1990}$ is somewhat lower than the loss in glacier area (35%) between 1850 and the 1970s as estimated from inventories by Zemp et al. (in press). This suggests that either the model is not perfectly able to reproduce the area loss between 1850 and the 1970s, or that a rise in temperature by 0.6 °C cannot completely explain the corresponding glacier shrinkage. In the $MR_{T+3/P+10}$ the 10% increase in precipitation compensates for only a small amount of the ELA_0 rise caused by the temperature rise of 3 °C. The average rise of the $rcELA_0$ of 336 m clearly exceeds the upper boundary of the approximated confidence interval, based on Eq. (4). As a consequence, many areas become ice-free. The cAA of the reference run is reduced by 74%. This relative area loss clearly indicates the dimension of such a change. These results correspond well with other studies that are based on different methods. Maisch et al. (2000) quote a glacier area loss in Switzerland of 75% for an ELA rise of 300 m. Haeberli and Hoelzle (1995) applied a parameterisation scheme to glacier inventory data to simulate potential climate change effects on Alpine glaciers. They expect a reduction of glacier area and volume to a few percent of the values estimated for the 1850 glacierisation by the second half of the 21st century.

5.3. Potential applications

The presented approach is a valuable complement to current distributed mass balance models (e.g., Klok and Oerlemans, 2002; Paul et al., in press). Since the distributed ELA_0-model needs only a minimum of input data, it is able to compute the $rcELA_0$ and the cAA over the entire Alps. Distributed mass balance models are (currently) not able to be applied to such large areas, but can be used for individual glaciers or within glacierised catchments to account for further important components of the energy balance (e.g., solar radiation, albedo, turbulent fluxes, mass balance–altitude feedback) and local, topographic effects (e.g., shading, avalanches, snow drift).

Eq. (1) has the potential to estimate precipitation at glacier locations when the glacier ELA_0 and the temperature at the ELA_0 are known. The example of Silvretta Glacier demonstrates that the presented approach is a promising tool for estimating precipitation in high altitude terrain. However, in doing so, one has to take into account the uncertainties, both of the model and of the reconstruction of the ELA_0. In addition, Eq. (1) seems to be plausible beyond the range of the parameters on which it is based (Fig. 10), but a future aim must be to enlarge this data set on an identical methodological basis. Here, availability and quality of the precipitation data at glacier ELA_0 will be the decisive element.

Regional climate models (RCM) have a horizontal resolution of about 20–50 km. These models use static glacier masks which indicate whether a specific grid cell is covered completely by ice or is totally ice-free. These glacier masks remain constant throughout the model simulation. Potential changes in the ice cover, their feedback to the atmosphere and their effects (e.g., enhanced summer runoff due to glacier melting) are not accounted for. Current efforts are undertaken to represent mountain glaciers in RCMs on a subgrid scale (Kotlarski and Jacob, 2005). Here, information on altitude-area distribution of glaciers for the initialisation of time-slice experiments and for model validation is urgently needed. Hence, quality and resolution of the approach presented here would definitely be good

enough to provide an approximation of glacier altitude-area distribution for past and present states as well as for future climate scenarios.

6. Conclusions

Based on direct glaciological mass balance measurements for the period of 1971–1990, this study presents an empirical relationship between 6-month summer temperature and annual precipitation at the glacier ELA_0. Using GIS techniques and a DEM (SRTM3), this relationship is applied for the first time to a distributed modelling of the $rcELA_0$ and the cAA over the entire Alps at a spatial resolution of 3 arc sec (approx. 100 m). It is shown that the altitude of the terrain is the decisive factor determining the spatial distribution of the $rcELA_0$, and hence also of the cAA, superimposed by the precipitation field and the temperature field at 2000 m a.s.l. The empirical relationship is able to explain about 50% of the variance in precipitation at the glacier ELA_0 by the variance in temperature at that location. Hence, the uncertainties in the prediction of precipitation based on a given temperature and the ELA_0 at a single location are rather large. Nevertheless, it represents a promising tool for the estimation of precipitation in high altitude terrain based on a large number of ELA_0 values. The empirical relationship is used as a boundary condition for the distributed modelling of the $rcELA_0$. The mean absolute difference between modelled $rcELA_0$ and measured ELA_0 amounts to about 70 m. The uncertainties of the $rcELA_0$ are restricted to its location, and affect the cAA only in flat terrain. Under the assumption that local, topographic effects and components of the energy balance not included in the model do not change, the distributed modelling approach presented here is an adequate tool for studies of glacier sensitivity to changes in temperature and/or precipitation.

A sensitivity study shows that a summer temperature deviation of ±1 °C results in an average deviation of the $rcELA_0$ of +137/−125 m. An annual precipitation deviation of ±25% (an order of magnitude of 300 mm) leads to a deviation of the $rcELA_0$ of −114/+157 m. A summer temperature decrease of 0.6 °C lowers the ELA_0 by 75 m on the Alpine average and by 65 m within the outlines (>1 km^2) of the 1973 Swiss Glacier Inventory. A summer temperature rise of 3 °C combined with an increase in annual precipitation of 10% results in an average rise in the $rcELA_0$ of 336 m and a reduction in the cAA in the order of 74%.

To enhance the statistical basis and to extend the range of validity of the empirical relationship, we recommend the determination of monthly, seasonal or at least annual precipitation and temperature at the ELA_0 of all glaciers with mass balance measurements. These two parameters together with the calculation of the ELA values should become a standard component of mass balance measurement series.

The presented approach is an excellent complement to distributed mass balance models. As the distributed $rcELA_0$-model requires only a minimum amount of input data to compute the $rcELA_0$ over the entire Alps, distributed mass balance models can then be used to account for further important components of the energy balance (e.g., solar radiation, albedo, turbulent fluxes, mass balance–altitude feedback) and local, topographic effects (e.g., shading, avalanches, snow drift) within individual catchments.

In conclusion, distributed modelling of the $rcELA_0$ can potentially contribute to the current efforts to include glacier altitude-area distribution of past, present and future glacier states in regional climate models.

Acknowledgements

We are indebted to the following institutes and organisations that placed their data at our disposal: Central Institute for Meteorology and Geodynamics in Vienna (temperature data), Institute for Atmospheric and Climate Science at the ETH in Zurich (precipitation data), Land Processes Distributed Active Archive Centre located at the U.S. Geological Survey in Sioux Falls (HYDRO1k), MeteoSwiss in Zurich (temperature data), National Aeronautics and Space Administration in Washington (SRTM3 and SRTM30), Swisstopo in Bern (DEM25L2), and World Glacier Monitoring Service in Zurich (mass balance measurements). Sincere thanks are given to the following colleagues for fruitful discussions and helpful comments in their research fields: Christoph Frei and Manfred Schwarb (precipitation and precipitation gradients in the European Alps), Sven Kotlarski (regional climate models), Frank Paul (DEM production and mass balance modelling), Max Maisch (Swiss glaciers), Nadine Salzman (climate modelling and interpolation techniques), Dominic Schuhmacher and the BABS group (statistical analysis). We gratefully acknowledge the constructive comments of Andrew G. Fountain, an anonymous referee and of the guest editor in charge Bruce Raup. Thanks go to Karen Hames and Susan Braun-Clarke for editing the English. The present study is funded mainly by the Swiss Federal Office of Education and Science (BBW-Contract 901.0498-2)

within the EU programme ALP-IMP (Contract EVK2-CT-2002-00148).

References

Ahlmann, H.W., 1924. Le niveau de glaciation comme fonction de l'accumulation d'humidité sous forme solide. Geografisk Annaler VI, 223–272.

Ananicheva, M.D., Krenke, A.N., 2005. Evolution of climatic snow line and equilibrium line altitudes in the north-eastern Siberia mountains (20th century). Ice and Climate News 6, 3–6.

Auer, I., Böhm, R., Jurkovic, A., Orlik, A., Potzmann, R., Schöner, W., Ungersböck, M., Brunetti, M., Nanni, T., Maugeri, M., Briffa, K., Jones, P., Efthymiadis, D., Mestre, O., Moisselin, J.M., Begert, M., Brazdil, R., Bochnicek, O., Cegnar, T., Gajic-Capka, M., Zaninovic, K., Majstorovic, Z., Szalai, S., Szentimrey, T., 2005. A new instrumental precipitation data set in the greater alpine region for the period 1800–2002. International Journal of Climatology 25/2, 139–166.

Braithwaite, R.J., 1981. On glacier energy balance, ablation and air temperature. Journal of Glaciology 27 (97), 381–391.

Braithwaite, R.J., Zhang, Y., 2000. Sensitivity of mass balances of five Swiss glaciers to temperature changes assessed by tuning a degree-day model. Journal of Glaciology 46 (152), 7–14.

Frei, C., Schär, C., 1998. A precipitation climatology of the Alps from high-resolution rain-gauge observations. International Journal of Climatology 18, 873–900.

Greene, A.M., Broecker, W.S., Rind, D., 1999. Swiss glacier recession since the Little Ice Age: reconciliation with climate records. Geophysical Research Letters 26 (13), 1909–1912.

Greuell, W., 1989. Glaciers and climate: energy balance studies and numerical modelling of the historical front variations of the Hintereisferner (Austria). Ph.D. Thesis, Utrecht University, Netherlands, 178 pp.

Gross, G., Kerschner, H., Patzelt, G., 1978. Methodische Untersuchungen über die Schneegrenze in alpinen Gletschergebieten. Zeitschrift für Gletscherkunde und Glazialgeologie 12 (2), 223–251.

Haeberli, W., 1983. Permafrost–glacier Relationships in the Swiss Alps Today and in the Past. Proceedings of the Fourth International Conference on Permafrost, Fairbanks AK. National Academy of Sciences, Washington, D.C., pp. 415–420.

Haeberli, W., 2004. Glaciers and ice caps: historical background and strategies of world-wide monitoring. In: Bamber, J.L., Payne, A.J. (Eds.), Mass Balance of the Cryosphere. Cambridge University Press, Cambridge, pp. 559–578.

Haeberli, W., Hoelzle, M., 1995. Application of inventory data for estimating characteristics of and regional climate-change effects on mountain glaciers: a pilot study with the European Alps. Annals of Glaciology 21, 206–212.

Hoinkes, H.C., Steinacker, R., 1975. Zur Parametrisierung der Beziehung Klima-Gletscher. Rivista Italiana di Geofisica e Scienze Affini 1, 97–104 (Speciale).

Hydrological Atlas of Austria, 2003. Bundesministerium für Land-und Forstwirtschaft, Umwelt und Wasserwirtschaft. Österreichischer Kunst-und Kulturverlag, Wien, Plate, vol. 2.2.

IPCC, 2001. Climate change 2001: the scientific basis. Contribution of working group I to the Third Assessment Report of the Intergovernmental Panel on Climate Change. Cambridge University Press, Cambridge, UK, 881 pp.

IUGG(CCS)/UNEP/UNESCO/WMO, 2005. In: Haeberli, W., Noetzli, J., Zemp, M., Baumann, S., Frauenfelder, R., Hoelzle, M. (Eds.), Glacier Mass Balance Bulletin No. 8 (2002–2003). World Glacier Monitoring Service, Zurich, 100 pp.

Kääb, A., Paul, F., Maisch, M., Hoelzle, M., Haeberli, W., 2002. The new remote-sensing-derived Swiss Glacier Inventory: II. First results. Annals of Glaciology 34, 362–366.

Kerschner, H., 1985. Quantitative paleoclimatic inferences from late glacial snowline, timberline and rock glacier data, Tyrolean Alps, Austria. Zeitschrift für Gletscherkunde und Glazialgeologie 21, 363–369.

Kerschner, H., 1996. Multivariate statistical modelling of equilibrium line altitudes. Hintereisferner (Ötztal)-Stubacher Sonnblickkees (Hohe Tauern). Zeitschrift für Gletscherkunde und Glazialgeologie 32, 119–127.

Kerschner, H., 2002. Mountain glaciers as sources of palaeoclimatic information — an alpine perspective. WMO Bulletin 51 (1), 29–35.

Kerschner, H., Kaser, G., Sailer, R., 2000. Alpine Younger Dryas glaciers as palaeo-precipitation gauges. Annals of Glaciology 31, 80–84.

Klok, E.J., Oerlemans, J., 2002. Model study of the spatial distribution of the energy and mass balance of Morteratschgletscher, Switzerland. Journal of Glaciology 48 (163), 505–518.

Kotlarski, S., Jacob, D., 2005. Development of a subgrid scale parameterization of mountain glaciers for use in regional climate modelling. WGNE Blue Book, WMO, pp. 4–13.

Krenke, A.N., 1975. Climatic conditions of present-day glaciation in Soviet Central Asia. IAHS-AISH 104, 30–41.

Kuhn, M., 1981. Climate and glaciers. IAHS 131, 3–20.

Letréguilly, A., Reynaud, L., 1990. Space and time distribution of glacier mass-balance in the northern hemisphere. Arctic and Alpine Research 22 (1), 43–50.

Leysinger Vieli, G.J., Gudmundsson, G.H., 2004. On estimating length fluctuations of glaciers caused by changes in climatic forcing. Journal of Geophysical Research 109, F01007, doi:10.1029/2003JF000027.

Lie, O., Dahl, S.O., Nesje, A., 2003a. A theoretical approach to glacier equilibrium-line altitudes using meteorological data and glacier mass balance records from southern Norway. The Holocene 13.3, 365–372.

Lie, O., Dahl, S.O., Nesje, A., 2003b. Theoretical equilibrium-line altitudes and glacier buildup sensitivity in southern Norway based on meteorological data in Geographical Information System. The Holocene 13.3, 373–380.

Lillesand, T.M., Kiefer, R.W., 1994. Remote Sensing and Image Interpretation, 3rd edition. Wiley & Sons, Inc., New York, 750 pp.

Maisch, M., 1992. Die Gletscher Graubündens. Rekonstruktion und Auswertung der Gletscher und deren Veränderungen seit dem Hochstand von 1850 im Gebiet der östlichen Schweizer Alpen (Bündnerland und angrenzende Regionen). Teil A: Grundlagen-Analysen-Ergebnisse. Physische Geographie, vol. 33. Geographisches Institut der Universität Zürich, Zurich, 324 pp.

Maisch, M., Wipf, A., Denneler, B., Battaglia, J., Benz, C., 2000. Die Gletscher der Schweizer Alpen. Gletscherhochstand 1850, Aktuelle Vergletscherung, Gletscherschwund Szenarien, Schlussbericht NFP31, 2nd edition. VdF Hochschulverlag, Zurich, 373 pp.

OcCC, 2004. Klimaentwicklung in der Schweiz bis 2050. Ein kurzer Überblick. Studie im Rahmen des Forschungsprogramms Energiewirtschaftliche Grundlagen des Bundesamts für Energie BFE, durchgeführt durch das Organe consultatif pour le Changement Climatique (OcCC), Bern, 7 pp.

Oerlemans, J., 2001. Glaciers and Climate Change. A.A. Balkema Publishers, Lisse, 148 pp.

Ohmura, A., Kasser, P., Funk, M., 1992. Climate at the equilibrium line of glaciers. Journal of Glaciology 38, 397–411.

Oliver, M.A., Webster, R., 1990. Kriging: a method of interpolation for Geographical Information Systems. International Journal of Geographical Information Systems 4 (3), 313–332.

Paul, F., Kääb, A., Maisch, M., Kellenberger, T.W., Haeberli, W., 2002. The new remote-sensing-derived Swiss Glacier Inventory: I. methods. Annals of Glaciology 34, 355–361.

Paul, F., Machguth, H., Hoelzle, M., Salzmann, N., Haeberli, W., in press. Alpine-wide distributed glacier mass balance modelling: a tool for assessing future glacier change? In: Orlove, B., Wiegandt, E., Luckmann, B. (Eds.), The darkening peaks: Glacial retreat in scientific and social context. University of California Press.

Rabus, B., Eineder, M., Roth, A., Bamler, R., 2003. The shuttle radar topography mission — a new class of digital elevation models acquired by spaceborne radar. ISPRS Journal of Photogrammetry and Remote Sensing 57 (4), 241–262.

Schwarb, M., Daly, C., Frei, C., Schär, C., 2001. Mean annual and seasonal precipitation throughout the European Alps 1971–1990. Hydrological Atlas of Switzerland. Plates 2.6, 2.7.

Sevruk, B., 1985. Systematischer Niederschlagsfehler in der Schweiz. Beiträge zur Geologie der Schweiz. Hydrologie, vol. 31. Kuemmerly and Frey, Bern, pp. 65–75.

Shea, J.M., Marshall, S.J., Livingston, J.L., 2004. Glacier distributions and climate in the Canadian Rockies. Arctic, Antarctic and Alpine Research 36 (2), 272–279.

Shumsky, P.A., 1964. Principles of structural glaciology. Translated from the Russian by D. Kraus. Dover Publications, Inc., New York, 497 pp.

Watson, D.F., Philip, G.M., 1985. A refinement of inverse distance weighted interpolation. Geo-Processing 2, 315–327.

Zemp, M., Paul, F., Hoelzle, M., Haeberli, W., in press. Glacier fluctuations in the European Alps 1850–2000: an overview and spatio-temporal analysis of available data. In: Orlove, B., Wiegandt, E., Luckmann, B. (Eds.), The darkening peaks: Glacial retreat in scientific and social context. University of California Press.